Evolution of the vibrational spectra of hydrogenated-amorphous-silicon thin films having columnar morphology

D. Masson,* E. Sacher, and A. Yelon

Groupe des Couches Minces et Département de Génie Physique, Ecole Polytechnique de Montréal, Case Postale 6079, succursale A, Montréal, Québec, Canada H3C 3A7

(Received 24 April 1986)

Columnar amorphous hydrogenated silicon (*a*-Si:H) has been prepared by microwave (2.45 GHz) discharge in Ar-SiH_4 mixtures using a large-volume microwave plasma apparatus. The films have been analyzed by Fourier-transform infrared spectroscopy, elastic recoil detection, and etching in both hydrofluoric and deuterofluoric acids. Time-dependent decreases in the intensities of the SiH_2 vibrational modes have been shown to occur at the same rates as the incorporation of atmospheric contaminants into the films. Elastic recoil detection and etching experiments suggest that the films evolve hydrogen at room temperature as they absorb atmospheric contaminants. These findings are used to offer a model for the loss of SiH_2 intensity.

I. INTRODUCTION

Hydrogenated amorphous silicon is usually prepared from silane using dc, audio-frequency, or radio-frequency plasmas. We report here on the ir spectra of samples which have been prepared in microwave discharges under conditions which lead to high levels of C and O contamination of the films, as well as to a columnar morphology.[1,2] Photomicrographs[2] of this morphology show the well-known fracture surface roughness which appears as columnlike structures 200—300 nm in diameter, extending from the substrate through to the surface of the deposited film. The SiH_n peaks of the infrared spectra of these films are essentially the same in position and shape as those of films which have neither columnar structure nor any appreciable amount of contaminants, indicating that the local environments of all these films are similar.

In a previous paper,[3] we showed that the infrared spectra of our microwave-deposited a-Si:H films evolved with time near room temperature. The main features of this evolution are decreases in the intensities of the SiH_2 absorption peaks near 2100 cm^{-1} (stretching), 896 cm^{-1} (bending), and 635 cm^{-1} (wagging), which followed the first-order kinetic rate equation

$$A_t^{\nu}=A_0^{\nu}\exp(-k^{\nu}t) , \quad (1)$$

where A_t^{ν} is the absorbance of the peak located at frequency ν at a time t after film deposition, A_0^{ν} is a constant and k^{ν} is the first-order rate constant for the process. These peaks are shown in Figs. 1 and 4 of Ref. 3 and all were found to evolve with the same kinetics.

In addition, an increase was seen in the intensities of a complex band in the 1200—800 cm^{-1} range, characteristic of bonding between Si and O, C, and N. In this paper, we present an analysis of the kinetics of that complex band of contaminants, as measured by Fourier-transform infrared (FTIR) spectroscopy. This analysis shows that the increasing contaminant peaks and the decreasing SiH_2 peaks evolve with similar rate constants. Elastic recoil detection (ERD) and etching measurements were also used, in an effort to clarify the mechanism of SiH_2 loss.

In particular, we address not only the time-dependent decreases of the SiH_2 peaks but why they are associated with identical increases in the contaminant-associated peaks. These new findings are examined in light of the possibilities suggested in our previous paper:[3] (1) the loss of singlet silylene trapped during deposition or (2) the onset of chemical reactions initiated by the contaminants. As we shall note, time-dependent processes also occur in noncolumnar material. We believe them to be the same as those occurring here, albeit at a far slower rate. Thus, the intentional fabrication of this material permits the evaluation of the kinetic rate processes of contamination, a study which would be impractical for the noncolumnar material.

II. EXPERIMENTAL

A. Materials preparation

The large-volume microwave plasma (LMP) generator previously described[4,5] has been used under conditions which intentionally produce thin films having columnar structure. The plasma generator operated at 2.45 GHz, using a SiH_4/Ar feed mixture at pressures of 4.7 and 21.6 Pa, respectively. An applied average power density of ≤ 0.1 W/cm^3 was used to deposit films onto crystalline Si substrates heated to 300 °C. Such conditions produced films about 1 μm in thickness for deposition times of 30 min, the thicknesses of our films being determined by profilometer, scanning electron microscope, and ERD profiles.

B. Characterization techniques

The IR spectrometer used was a Nicolet series 6000 FTIR which operated at a resolution of 3 cm^{-1} with an estimated signal-to-noise (S:N) ratio of approximately 40. This value of S:N was too low to permit the use of the ac-

 ©1987 The American Physical Society

companying software to deconvolute the peaks. Instead, deconvolution was accomplished with the older baseline and visual techniques. We note that the various peaks observed in our samples evolved at different rates. Thus, the subtraction of the absorption spectra obtained at different times following the preparation was used to identify the positions and shapes of the time-dependent absorption peaks. The reproducibility of the envelope from its components was always very good, as judged visually.

The ERD nuclear scattering technique described previously[4–6] was employed to study the hydrogen profile of an *a*-Si:H film over a period of two days following preparation. In this technique, a beam of ^{35}Cl is used to forward scatter the hydrogen and other light elements, which were then mass and energy analyzed. Spectral deconvolution leads to depth profiles of these light elements. In order to compare the results obtained by ERD with those obtained by infrared spectroscopy, a freshly prepared film was broken into two parts, which were simultaneously studied by ERD and FTIR at similar intervals of time subsequent to fabrication. This technique is not influenced by the morphology of the sample

The etching of our films, after their evolution had terminated, was carried out in 20 volume percent hydrofluoric and deuterofluoric acids, diluted in H_2O and D_2O, respectively. The samples were thoroughly rinsed in diluent, following those treatments. Their infrared spectra were obtained prior to and immediately after etching.

III. RESULTS

A. Infrared analysis of the evolution of the contaminant peaks

The kinetics of the evolution of the SiH_n peaks have already been reported.[1,3] The dominant feature is the first-order decrease of the peak intensity of the SiH_2 stretching mode at 2100 cm^{-1}, A_t^{2100}, to a nonzero final value, A_∞^{2100}. The intensity of the SiH_2 bending mode, A_t^{896}, decreases to zero in the same time interval and with the same kinetics, as does the weaker intensity wagging mode, A_t^{635}. The improved statistics provided by the accumulation of further data have permitted us to more precisely calculate $\Delta H^\ddagger$ and $\Delta S^\ddagger$, the enthalpy and entropy of activation, respectively, in the temperature range 20–57 °C. These values are found in Table I.

Over the same observation period, contamination peaks in the 1200–800 cm^{-1} region developed and grew. We were able to follow closely the growth of these peaks by successively subtracting the infrared spectra obtained on any given sample at various times. Figure 1 shows the difference of two ir spectra of the same sample taken 2 and 10 h after its preparation. We observe an increase of peaks centered around 1000 and 800 cm^{-1}, as well as the decrease of the SiH_2 bending mode, which appears as an inverted peak at 896 cm^{-1}. Figure 2 shows the difference of two ir spectra obtained on the same sample at times of 22 and 66 h after its preparation. The examination of many difference spectra, such as those illustrated in Figs. 1 and 2, has revealed the presence of four dominant peaks in that spectral region. By assuming a Gaussian shape to

TABLE I. Activation parameters for various time-dependent infrared absorption peaks.

Peak (cm^{-1})	$\Delta H^\ddagger$(kJ/mol)	$\Delta S^\ddagger$(J/mol K)
2100	92±7	−44±20
1112	90±10	−50±30
1056	56±10	−170±50
1000	92±7	−44±20

those four peaks, located at 1180, 1112, 1056, and 1000 cm^{-1}, and with full widths at half maxima (FWHM) of 50, 100, 90, and 90 cm^{-1}, respectively, we have been able to reproduce the undeconvoluted 1200–1000 cm^{-1} region at all stages of the evolution. The deconvoluted peaks are represented by dashed lines in Figs. 1 and 2, along with those in the 800–900 cm^{-1} range, discussed below.

The absorption sites responsible for the multiple peaks found in the 1000 cm^{-1} region are not yet known. Bonding between Si and O, C, and N atoms is known to produce absorptions in this region from stretching vibrational modes.[7,8] Generally, such bonds also have less intense bending-mode absorption peaks around 800 cm^{-1}. We have observed (see Figs. 1 and 2) peaks in that region, whose time-dependent intensities correlate well with those of the more intense stretching peaks. Thus, the peaks at 1112, 1056, and 1000 cm^{-1} have corresponding bending peaks at 880, 840, and 800 cm^{-1}, respectively. Linear correlations of the intensities of these pairs of peaks during their evolution show a typical correlation coefficient of 0.96 for about fifty pairs of experimental points.

The peak located at 1180 cm^{-1} did not have a counterpart in the 800 cm^{-1} region but, instead, was correlated with the growth of a peak at 460 cm^{-1}. The linear fit between the intensities of those two peaks also showed a good correlation coefficient, 0.97, for 20 points.

The kinetics of the evolution of the contaminant peaks situated at 1112, 1056, and 1000 cm^{-1} have been fitted to a first-order kinetic rate equation of the type:

$$A_t^\nu = A_\infty^\nu [1 - \exp(-k^\nu t)] , \quad (2)$$

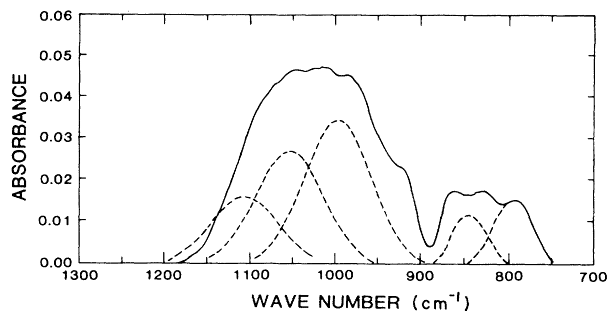

FIG. 1. Difference spectrum for a sample held at 43 °C, taken 10 and 2 h after deposition. The dotted lines are the deconvoluted peaks. A contaminant peak at approximately 880 cm^{-1} is not shown to avoid confusion with the inverted peak at 896 cm^{-1}. The inverted peak at 896 cm^{-1} is due to the decrease of the SiH_2 bending mode early in the evolution.

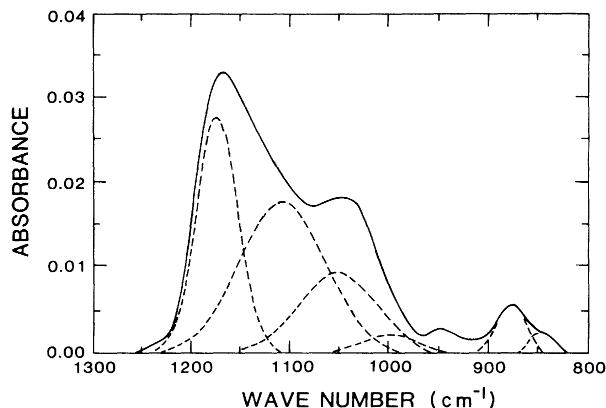

FIG. 2. Difference spectrum for the same sample shown in Fig. 1, taken 66 and 22 h after deposition. The dotted lines are the deconvoluted peaks.

where A_t^{ν} is the absorbance of the peak located at a frequency ν at a time t after deposition of the film, A_{∞}^{ν} is a constant, and k^{ν} is the first-order rate constant for the process. Figure 3 illustrates this for the contaminant peak at 1056 cm^{-1}, for samples studied at temperatures of 20, 31, 43, and 57 °C. Their $\Delta H^{\ddagger}$ and $\Delta S^{\ddagger}$ values are found in Table I, where a comparison with those for the SiH_2 stretching peak at 2100 cm^{-1} reveals that the contaminant peaks at 1112 and 1000 cm^{-1} have identical values.

For example, Fig. 4 demonstrates that the decrease of the SiH_2 stretching peak is well correlated with the increase of the deconvoluted contaminant peak at 1000 cm^{-1}. This linear relation persists when the parameters used for the deconvolution, (the position and FWHM of each peak) are changed within ranges corresponding to their uncertainties. This strongly suggests that the increases of the contamination peaks at 1112 and 1000 cm^{-1} are related to the decrease of the SiH_2 stretching peak at 2100 cm^{-1}.

The contaminant peaks at 1180 and 460 cm^{-1} did not follow simple first-order kinetics. Instead those peaks ap-

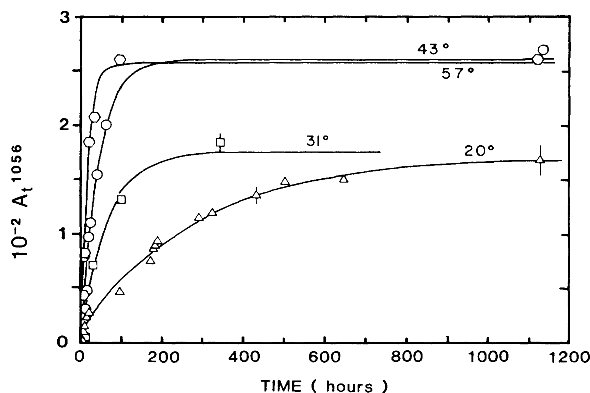

FIG. 3. Peak height of the deconvoluted peak at 1056 cm^{-1} for four similar LMP samples held at 20, 31, 43, and 57 °C as a function of time. The solid lines represent the best fit of the experimental points to Eq. (1).

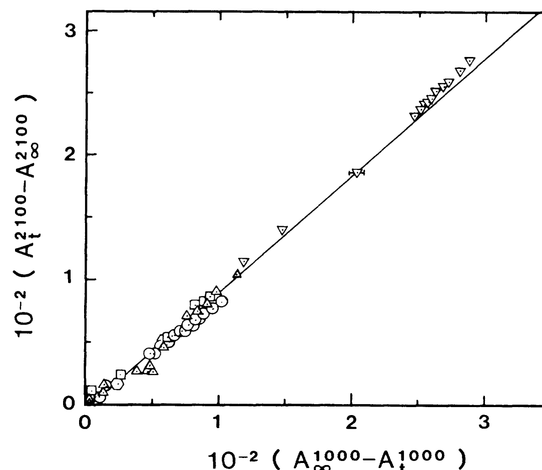

FIG. 4. Correlation between the decrease of the SiH_2 stretching peak at 2100 cm^{-1} and the increase of the deconvoluted peak at 1000 cm^{-1} during the evolution. The different symbols refer to samples whose evolution took place at different temperatures (20 to 60 °C). The correlation coefficient was 0.996.

peared in the infrared spectra after the other contaminant peaks had reached about half of their final heights (see Fig. 6 of Ref. 2), suggesting that they are caused by the agglomeration of contaminants.

In Fig. 5 we have plotted the final absorbances, A_{∞}^{ν}, for $\nu=1112$ and 1056 cm^{-1}, as a function of sample thickness. We observe a trend such that the absorbances of those two peaks seem to saturate for thicknesses larger than approximately 0.5 μm. In contrast, the contaminant peak at 1000 cm^{-1} followed a linear relationship with thickness to the largest thicknesses measured, as did the SiH_2 stretching peak. It thus appears that the contaminations indicated by the peaks at 1112 and 1056 cm^{-1} are confined to surface layers.

B. Comparison of the loss of hydrogen measured by infrared absorption and ERD

The hydrogen profiles obtained by ERD on a 1.3 μm thick sample are shown in Fig. 6. These spectra were ob-

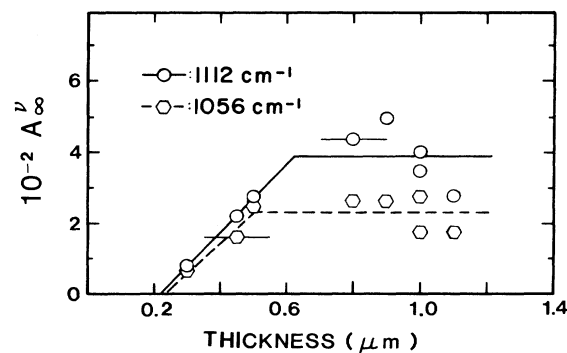

FIG. 5. Peak heights of the deconvoluted contaminants peaks at 1112 and 1056 cm^{-1}, after evolution had ceased, versus sample thickness.

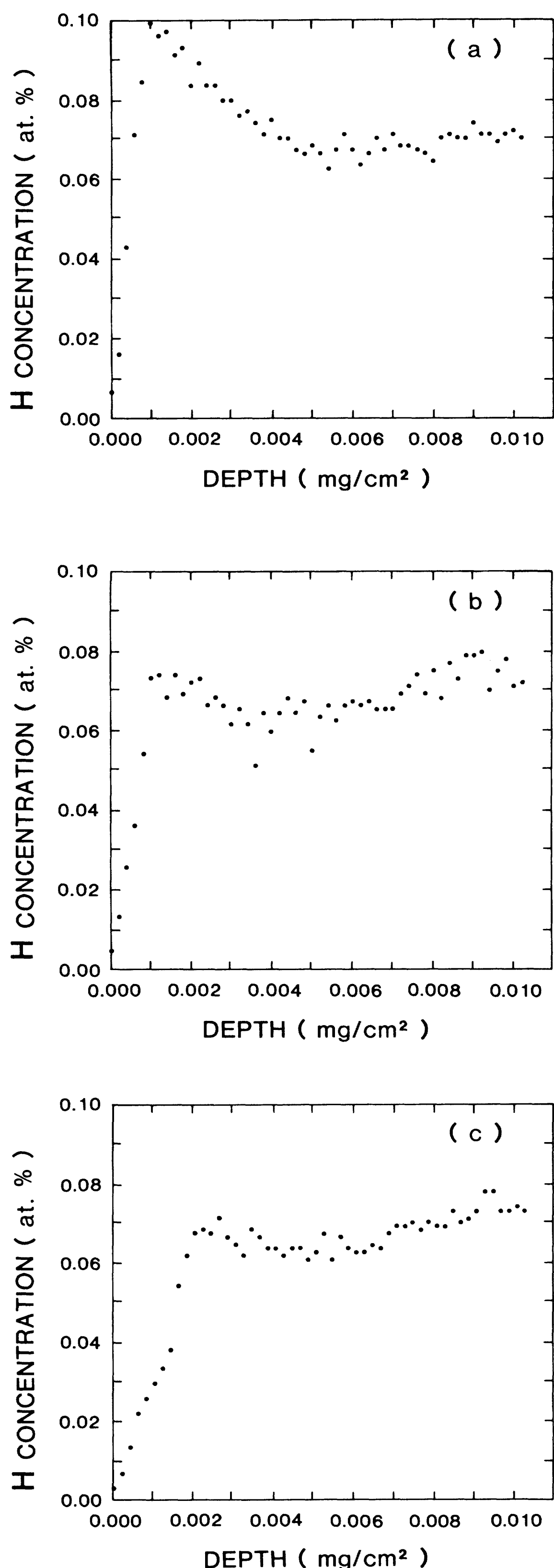

FIG. 6. Hydrogen profiles determined by ERD as a function of time: (a) 2, (b) 18, and (c) 42 h after the fabrication. The sample was at ambient temperature during the ERD scans.

TABLE II. Comparison of the loss of hydrogen by ERD and infrared absorption.

Time (h)	$\left[\frac{(\Delta N_H)_t}{(N_H)_{t=2}}\right]_{ERD}$	$\left[\frac{(\Delta N_H)_t}{(N_H)_{t=2}}\right]_{ir}$
18	0.050±0.003	0.049±0.004
42	0.076±0.004	0.085±0.004

tained 2, 18, and 42 h after deposition. We observe, in that period, a loss of hydrogen within a distance of about 0.4 μm from the outer surface, whereas, below 0.4 μm, the hydrogen content remains constant. One notes that this surface layer thickness corresponds roughly to that of the surface layer contaminants.

In Table II, we have listed the relative loss of hydrogen, $\Delta(N_H)_t/(N_H)_{t=2}$, as computed from the integrals of the hydrogen concentration curves of Fig. 6. The concentration of hydrogen beyond 0.6 μm, not shown in Fig. 6, was taken to be constant at a value given by the average of the H concentration before 0.6 μm. Table II also contains the relative loss of Si-bonded hydrogen computed from the integrated infrared stretching bands, on the same sample, at identical times after deposition (the sample had been broken into two parts after deposition). This calculation of the loss of hydrogen is valid, provided that the oscillator strengths of all the SiH_n stretching modes are nearly identical, as is the case for silane gas.[9] The average oscillator strength of the SiH_n stretching modes of our films was found, from FTIR and ERD, to be 4.2 cm^2/m mol, in good agreement with previously published proportionality constants.[9–11]

By comparing the loss of hydrogen in this way, we eliminate any errors that might arise due to the uncertainties in the values of both the oscillator strength and the sample thickness. Therefore, the uncertainties in the values listed in Table II are uniquely due to the uncertainties in the evaluation of the integrals of the ERD and infrared spectra. This confirmation of the hydrogen loss by two distinctly different methods strongly supports the view that hydrogen has evolved from the film.

C. Etching

A few samples were subjected to chemical attack in either HF or DF solutions after their spectra had stopped

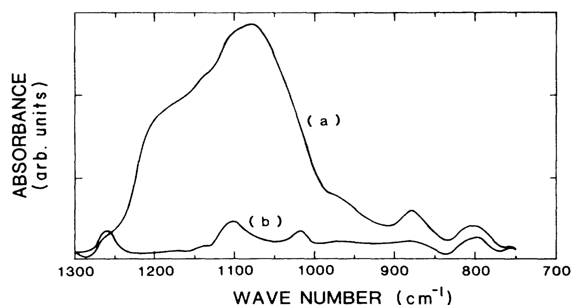

FIG. 7. Absorption due to contaminants (a) after an exposure of the sample to ambient air for several months and (b) after etching in DF.

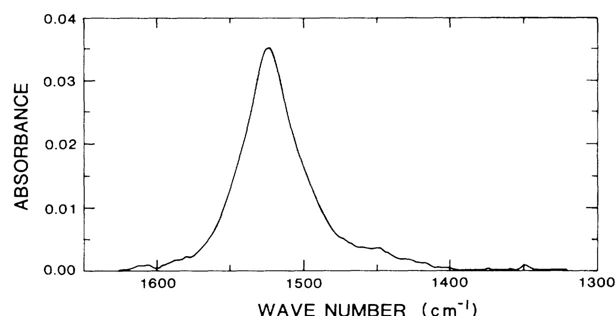

FIG. 8. Difference spectra showing the growth of the SiD_2 stretching peak after etching in DF.

changing (a few months after their preparation). An etching time of 30 sec was sufficient to remove all the contaminant absorption peaks in the 1200—800 cm^{-1} region, as well as the 460 cm^{-1} peak. This is shown in Fig. 7.

The second effect of this chemical attack was the reappearance of SiH_2 peaks when HF was used and the introduction of a peak at 1524 cm^{-1} when DF was used. Figure 8 shows the peak at 1524 cm^{-1}. The ratio of the SiH_2 stretching frequency, 2100 cm^{-1}, to that of the peak at 1524 cm^{-1} (1.38) agrees well with the square root of the ratio of the reduced masses of SiD_2 and SiH_2 (1.39). This suggests that the peak at 1524 cm^{-1} is due to the SiD_2 stretch. Confirmation is provided by the appearance of a less intense peak at 650 cm^{-1} which agrees well with the square root of the reduced mass factor for the SiH_2 bending frequency (896 cm^{-1}). Brodsky *et al.*[9] and Freeman and Paul[10] found values of 1.39 and 1.37, respectively, for their SiD_n peak shifts.

By comparing the areas under the appropriate peaks, the amount of SiH_2 or SiD_2 which was formed after the etching was found to be 85% of the concentration of SiH_2 sites that appeared immediately after deposition. The SiH peak at 2000 cm^{-1}, which remained essentially stable during the evolution (showing variations of about 0.05 of its initial height), was not affected by these treatments. Futhermore, no traces of SiD or SiHD stretching peaks were found after etching in DF. Following etching, the time-dependent process was seen to start anew; a decrease in the SiH_2 (or SiD_2) peaks was accompanied by an increase in the contaminant peaks around 1000 cm^{-1}, previously shown to be due to bulk contamination. The decrease once more followed first-order kinetics but the rate was about 3 times slower than the rate observed immediately after sample preparation.

IV. DISCUSSION

A. Contaminant peaks (1200—800 cm^{-1})

LMP samples have a columnar morphology, which is known to have a higher concentration of free radicals[12] than radio-frequency (13.56 MHz) samples and, hence, a greater ability to adsorb some contaminants; we find about 3% C and 4% O. Samples made under similar conditions of cleanliness but with the more conventional radio-frequency plasma system did not show columns and showed much lower levels of C and O.[1] The time dependence of infrared absorption peaks in the region where Si, singly bonded to C, O, and N, is known to absorb (~ 1100 cm^{-1}) (Refs. 6 and 7) confirms that atmospheric contaminants penetrate our LMP films and this, over periods of up to several weeks after the fabrication. A close look at the evolution of that spectral region reveals that many peaks and, therefore, many contaminant sites, are present in our LMP films.

B. SiH_2 stretching peak

We had initially proposed[2] that the extremely stable[13] singlet silylene (:SiH_2), known to be present in the plasma,[14,15] could be trapped in voids in the film. Its loss could account for the decrease of the SiH_2 peaks. Whatever the proposed mechanism which might be responsible for the loss of hydrogen from SiH_2 sites, it must be compatible with the following:

(1) We have observed a linear relation between the decrease of the SiH_2 peaks and the increase of certain contaminant peaks, suggesting that contamination plays a role in the disappearance of this peak.

(2) The values of $\Delta H^{\ddagger}$ and $\Delta S^{\ddagger}$ found for the decrease of the SiH_2 stretching peaks are such that, at 300 °C (which is the temperature of the sample immediately after the preparation), the time dependence of those peaks should have been over within a fraction of a second. This strongly supports our view that subsequent reaction with atmospheric contaminants plays a role in the decrease of the SiH_2 peak.

(3) We have not observed the growth of peaks that might indicate that the SiH_2 hydrogens could have been transferred to other sites during the evolution (e.g., OH, NH). We have seen CH_n peaks but their evolution does not suggest any relation with the decrease of the SiH_2 peaks.

(4) The loss of hydrogen, as determined by ERD, is well correlated with that determined by the integrated SiH_2 stretching peak, as well as with the layer thickness occupied by the surface layer contaminants. Further, the kinetics of SiH_2 loss and 1200 cm^{-1} contaminant growth were identical. This suggests that hydrogen from those sites actually leaves our films during the evolution.

(5) After etching in HF (or DF), the evolution was seen to begin anew; the SiH_2 (or SiD_2) peaks which appeared after the etching were seen to decrease as contaminants peaks in the 1000 cm^{-1} region (cleaned by the etching) grew once more. The SiH peaks remained unchanged.

The diffusion of silylene out of the sample would explain points 3 and 4 above. It does not, explain points 1 and 2 in a straightforward manner and could hardly be reconciled with point 5. Therefore, the diffusion of silylene out of our samples as a mechanism for the decrease of the SiH_2 peaks appears inadequate. Furthermore, the stability of singlet silylene in an *a*-Si:H structure is probably insufficient to account for the half-life (approximately 6 d) observed in the first-order decrease of the SiH_2 peaks at room temperature.[16]

The diffusion of atmospheric contaminants into our

films appears to play an important role, as yet unknown, in the time-dependent loss of SiH_2 sites. Indeed, we might imagine a process through which some contaminants penetrate the columnar structure of our films and react with the SiH_2, with a simultaneous loss of hydrogen. In the following subsection, we offer a possible mechanism for the initiation of this process.

C. Time-dependent processes in *a*-Si:H

Studies in our laboratory have demonstrated the existence of time-dependent ir spectral changes in non-columnar *a*-Si:H films. These changes were manifested by reductions in Si-H_n vibrational peak heights, increases in contaminant peak heights and chemical shifts, as in the present results. They were, however, very slow, occurring over a period of years. It was these findings which prompted us to search for samples which exhibited changes over a time scale short enough to be used for kinetic determinations, as in the present study.

There is evidence that both plasma-deposited[10] and solution-deposited[17–19] *a*-Si:H prepared by other workers show contamination and changes in Si-H_n peaks when exposed to the atmosphere. The data of Freeman and Paul,[10] taken on plasma-deposited material over the complete spectral range of 200–4000 cm^{-1}, are remarkably similar to our own, showing the same changes in Si-H_n and contaminant peaks. Those of John and coworkers,[17–19] taken on solution-deposited material, are confined to the Si-H_n peaks; they are, however, similar to our spectra. As recently noted,[20] these findings are almost identical to those obtained when oxygen is intentionally incorporated during the fabrication process.[7,10,11,21–24].

The reactions occurring in these films are complex and, as shown here, involve the making and breaking of bonds, as well as the migration of chemical species. They have only begun to be sorted out. The question of which contaminants penetrate, to serve as reactants for this process, can be considered in a more straightforward manner:[20,25] both oxygen and carbon have been found to contribute to subsurface contamination, while a hydrocarbon layer has been detected on the surface.

One may effectively eliminate water as a source of oxygen because of the absence of OH peaks in the spectra: both ir (Refs. 26 and 27) and election-energy-loss spectroscopy (EELS) (Ref. 28 and 29) show such peaks under conditions where water reacts with silicon surfaces. Carbon monoxide may also be eliminated, based on[20] orbital requirements for $p\pi$-$d\pi$ interactions, as well as the absence of ir peaks expected for CO reaction. Based on the similarity of contaminated and oxygenated *a*-Si:H spectra, as well as the presence of carbon, it appears that there are two penetrants: O_2 and the ubiquitous hydrocarbons in the atmosphere. In support of the ability of these hydrocarbons to contaminate, a recent EELS review[30] has noted that hydrocarbons react with activated surfaces through the making and breaking of bonds, to give the surface hydrocarbon layers previously found[25] on *a*-Si:H surfaces. Further, they confirm the presence of reactive vinyl unsaturation [peaks at 1440 and 1840 cm^{-1} (Ref. 31)] previously found by Stein.[32,33]

V. CONCLUSIONS

Our *a*-Si:H films, prepared in microwave discharges under conditions which intentionally give columnar morphology, were found to exhibit time-dependent ir spectral changes. The SiH_2 sites at 2100, 896, and 635 cm^{-1} all decreased with the same kinetic rates although that at 2100 cm^{-1} had a nonzero final value. At the same time, contaminant peaks, due to Si bonded to O, N, and C, began to grow in the 1200–800 cm^{-1} region. Those at 1112 (surface contamination) and 1000 (bulk contamination) cm^{-1} had the same kinetics as the SiH_2 peaks, indicating that they are related.

The decrease in SiH_2 peaks appears to be due to a loss of hydrogen. This is demonstrated by ERD hydrogen profiles, which show a progressive loss of hydrogen from the sample surface. This loss correlates exactly with that calculated from the diminution of the ir peaks. Etching in HF removes the contaminant peaks and reintroduces SiH_2 peaks, whereupon the time-dependent processes begin anew.

Our results are consistent with a model in which contaminants penetrate a columnar film, with O_2 and hydrocarbon contaminants reaching only a limited depth. Reaction with the amorphous silicon leads to the breaking of SiH_2 bonds, loss of hydrogen, and the incorporation of the contaminants into the matrix. Etching with HF removes these structures, reintroducing SiH_2 bonds. While the nature of the detailed reactions is presently unknown, the similarity of the present results to those found for non-columnar material makes it likely that the reactions found here occur in all *a*-Si:H material, the principal difference lying in the speed with which they occur.

ACKNOWLEDGMENTS

The authors wish to thank Professor Ian Butler for the use of his FTIR and the Natural Sciences and Engineering Research Council (NSERC) of Canada and the Fonds FCAR pour l'Aide et le Soutien à la Recherche du Gouvernement du Québec (Québec, Canada) for funding.

---

*Present address: School of Applied and Engineering Physics, Cornell University, Clark Hall, Ithaca, NY 14853-2501.

[1]L. Paquin, J. F. Currie, B. Noirhomme, S. Poulin-Dandurand, E. Sacher, M. R. Wertheimer, A. Yelon, J. L. Brebner, R. W. Cochrane, R. Groleau, H. Lu, and J. P. Martin, Proceedings of the 6th International Symposium on Plasma Chemistry, 1983 (unpublished), p. 787.

[2]L. Paquin, D. Masson, M. R. Wertheimer, and M. Moisan, Can. J. Phys. **63**, 831 (1985).

[3]D. Masson, L. Paquin, S. Poulin-Dandurand, E. Sacher, and A. Yelon, J. Non-Cryst. Solids **66**, 93 (1984).

[4]J. F. Currie, P. Depelsenaire, J. P. Huot, L. Paquin, M. R.

Wertheimer, A. Yelon, C. Brassard, J. L'Ecuyer, R. Groleau, and J. P. Martin, Can. J. Phys. **61**, 582 (1983).

[5]C. Mailhot, J. F. Currie, S. Sapieha, M. R. Wertheimer, and A. Yelon, J. Non-Cryst. Solids **35**, 207 (1980).

[6]J. F. Currie, P. Depelsenaire, R. Groleau, and E. Sacher, J. Coll. Interface Sci. **97**, 410 (1984).

[7]G. Lucovsky, J. Yang, S. S. Chao, J. E. Tyler, and W. Czubatyj, Phys. Rev. B **29**, 2302 (1984).

[8]N. B. Colthup, L. H. Daly, and S. E. Wiberly, *Introduction to Infrared and Raman Spectroscopy,* 2nd ed. (Academic, New York, 1975), p. 294.

[9]M. H. Brodsky, M. Cardona, and J. J. Cuomo, Phys. Rev. B **16**, 3556 (1977).

[10]E. C. Freeman and W. Paul, Phys. Rev. B **18**, 4288 (1978).

[11]G. Lucovsky, J. Yang, S. S. Chao, J. E. Tyler, and W. Czubatyj, Phys. Rev. B **28**, 3225 (1983).

[12]J. C. Knights, G. Lucovsky, and R. J. Nemanich, J. Non-Cryst. Solids **32**, 393 (1979).

[13]P. P. Gaspar, S. Konieczny, and S. H. Mo, J. Am. Chem. Soc. **106**, 424 (1984).

[14]G. Turban, Y. Catherine, and B. Grolleau, Thin Solids Films **77**, 287 (1981).

[15]G. Turban, Y. Catherine, and B. Grolleau, Plasma Chem. Plasma Proc. **2**, 61 (1982).

[16]P. P. Gaspar (private communication).

[17]P. John, I. M. Odeh, M. J. K. Thomas, and J. I. B. Wilson, J. Phys. (Paris), Colloq. **42**, C4-651 (1981).

[18]P. John, I. M. Odeh, M. J. K. Thomas, M. J. Tricker, and J. I. B. Wilson, Phys. Status Solidi B **105**, 499 (1981).

[19]P. Vora, S. A. Solin, and P. John, Phys. Rev. B **29**, 3423 (1984).

[20]E. Sacher, Solar Energy Mater. **13**, 441 (1986).

[21]A. C. Adams, F. B. Alexander, C. P. Capio, and T. E. Smith, J. Electrochem. Soc. **128**, 1545 (1981).

[22]G. Lucovsky, Solar Energy Mater. **8** 165 (1982).

[23]G. Lucovsky and W. B. Pollard, J. Vac. Sci. Technol. **A1**, 313 (1982).

[24]G. Lucovsky, S. S. Chao, J. Chang, J. E. Tyler, and W. Czubatyj, J. Non-Cryst. Solids **66**, 99 (1984).

[25]E. Sacher, J. Klemberg-Sapieha, M. R. Wertheimer, H. P. Schreiber, and R. Groleau, Philos. Mag. B **49**, L47 (1984).

[26]Y. Chabal, Phys. Rev. B **29**, 3677 (1984).

[27]Y. Chabal, J. Vac. Sci. Techol. **A3**, 1448 (1985).

[28]J. A. Schaefer, D. Frankel, F. Stucki, W. Göpel, and G. J. Lapeyre, Surf. Sci. **139**, L209 (1984).

[29]F. Stucki, J. Anderson, G. J. Lapeyre, and H. H. Farrell, Surf. Sci. **143**, 84 (1984).

[30]N. Sheppard, J. Electron Spectrosc. Relat. Phenom. **38**, 175 (1986).

[31]L. J. Bellamy, *The Infrared Spectra of Complex Molecules* (Wiley, New York, 1959), p. 34.

[32]H. J. Stein, J. Electron. Mater. **4**, 159 (1975).

[33]H. J. Stein, Phys. Rev. Lett. **43**, 1030 (1979).